Физика

УДК 538.911 **DOI: 10.14529/mmph240208**

MAGNETIC AND STRUCTURAL PROPERTIES OF ALL-D METAL MN-NI-TI HEUSLER ALLOYS

***V.V. Sokolovskiy*[1], *V.D. Buchelnikov*[1], *D. Cong*[2]**
[1]*Chelyabinsk State University, Chelyabinsk, Russian Federation*
[2]*Beijing University of Science and Technology, Beijing, China*
E-mail: vsokolovsky84@mail.ru

Abstract. The paper presents a theoretical study of the effect of different atomic and magnetic orderings on the structural and magnetic properties of $Mn_2Ni_{1+x}Ti_{1-x}$ alloys, which are composed entirely of transition metals. Using the density functional theory, we predict the structural ground states and magnetic reference states of compounds with x = 0, 0,25, 0,5, and 0,75 in both cubic austenite and tetragonal martensite phases. Partial substitution of Ti atoms with Ni leads to an increase in the energy barrier between structural phases, to a change from a layered atomic ordering to an alternating staggered order, and to a change from antiferromagnetic to ferromagnetic spin alignment in the cubic phase. All compounds with tetragonally distorted structures reveal the out-of-plane spin configuration and easy axis magnetocrystalline anisotropy except tetragonal $L1_0$ phase of Mn_2NiTi. For the latter structure, easy-plane magnetic anisotropy is observed. The calculated values of anisotropy are comparable with those of tetragonal $L1_0$-FeNi.

Keywords: ab initio calculations; all-d metal Heusler alloys; atomic arrangement; magnetocrystalline anisotropy.

Introduction

In recent years, Ni-Mn ferromagnetic shape memory alloys have been extensively researched for commercial applications owing to their diverse multifunctional characteristics, including the magnetic shape memory effect, magnetocaloric effect, and magnetoresistance arising from temperature- or magnetic field-induced martensitic transformations [1–6]. However, challenges related to poor mechanical durability and significant hysteresis losses during phase transitions limit their practical application.

Recently, Heusler alloys have been developed that contain all *d*-transition metal elements based on nickel (Ni), manganese (Mn), and titanium (Ti) [7–9]. In these alloys, Ti replaces the elements from the *p*-block, and it has been shown that the *d*-block Ti metal provides stabilization of the Heusler structure through *d-d* hybridization with its nearest neighbor element [10]. These alloys exhibit an ordered $L2_1$ structure and an partially disordered B2 structure, and they undergo a phase transition from B2 to $L2_1$, which is accompanied by a change in structural order and a martensitic transformation at a lower temperature. In the B2 phase, some Mn atoms exchange positions with Ti atoms, leading to a strong antiferromagnetic interaction between Mn atoms located at different crystallographic sites.

A distinguishing feature of all-*d* metal Heusler alloys is their large relative volume change during the martensitic transformation process, which is significantly greater than in any other ferromagnetic shape memory alloy. This characteristic indicates a notable sensitivity of the transformation to applied mechanical stresses, particularly hydrostatic pressure. This makes these materials well-suited for demonstrating significant barocaloric effects. For example, Wei *et al.* [11] showed that a compressive stress of 900 MPa results in a deformation of approximately 3,9 % and an adiabatic temperature change of 10,7 K in $Ni_{50}Mn_{32}Ti_{18}$ alloy. Yan *et al.* [12] observed large deformations of approximately 13 % in the $Ni_{50}Mn_{31,75}Ti_{18,25}$ alloy under a compressive stress of 1,1 GPa. Due to the weaker *d-d* orbital hybridization in transition metal elements, there is a notable enhancement in mechanical properties, particularly improved plasticity, compared to conventional Heusler alloys that contain main group elements in combination with a strong *p-d* orbital interaction.

In this paper, we paid attention to the theoretical study of the effect of atomic ordering on the structural and magnetic characteristics of $Mn_2Ni_{1+x}Ti_{1-x}$ alloys within the framework of density functional theory.

1. Details of calculations

The calculations presented in this paper were performed within the framework of density functional theory, using the projection-augmented wave (PAW) method, which is implemented in the VASP software package [13, 14]. A series of $Mn_2Ni_{1+x}Ti_{1-x}$ Heusler alloys, consisting entirely of transition metals, were selected as the objects of study. The exchange-correlation energy approximation was realized using the generalized gradient approximation for electron density in the Perdew–Burke–Ernzerhof parametrization [15]. The following valence electron configurations were considered in the PAW potentials: $3s^2 3p^6 4s^2 3d^5$ for Mn, $3p^6 3d^8 4s^2$ for Ni, and $3s^2 3p^6 4s^2 3d^2$ for Ti. The plane wave basis cutoff energy was set at 450 eV, and a Monkhorst-Pack grid with a size of 8×8×8 was used for integration over the Brillouin zone. Geometric optimization of the 16 atom cells with cubic ($L2_1$, *Fm*3*m*, No. 225, and XA, *F*-43*m*, No. 216) and tetragonal (T^p, *P*4/*nmm*, No. 129) symmetries was performed using atomic position relaxation at constant volume and cell shape, with convergence criteria for energy and force equal to 10^{-6} eV and 10^{-2} eV/Å, respectively. Nonstoichiometric compounds were created by sequentially replacing Ti atoms with Ni. The following magnetic configurations were considered for the spin ordering of Mn atoms (see fig. 1): FM (ferromagnetic state), AFM (antiferromagnetic state with staggered arrangement of magnetic moments), and AFM* (antiferromagnetic layer-like arrangement of magnetic moments).

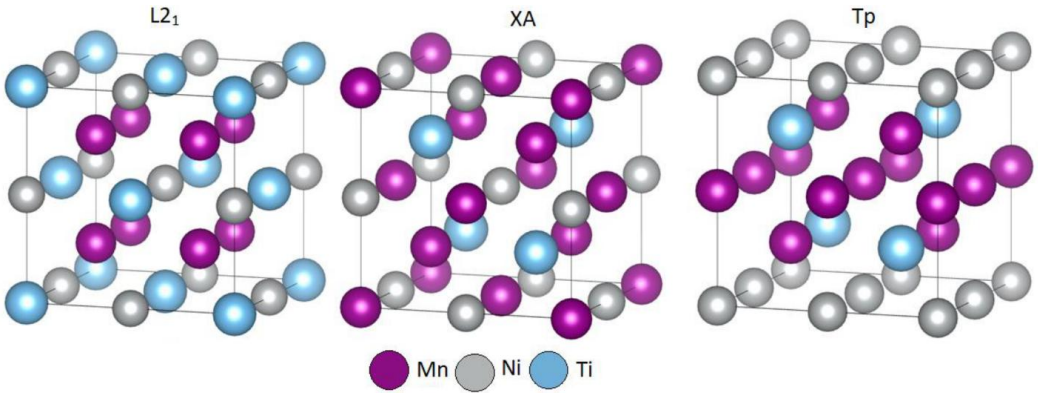

Fig. 1. The crystal structures of Mn_2NiTi Heusler alloy with cubic ($L2_1$, *Fm*3*m*, #225, and XA, *F*-43*m*, #216) and tetragonal (T^p, *P*4/*nmm*, #129) symmetry. The $L2_1$ and XA structures differ due to the placement of Mn atoms in equivalent and non-equivalent positions, respectively. The T^p structure is based on the XA structure and composed of layers of Mn and Ni atoms alternating along the [001] direction [16, 17]

The magnetocrystalline anisotropy energy (MAE) was calculated by performing successive self-consistent calculations that took into account spin-orbit interaction for structures with magnetic moment orientations along [001] and [100]. The MAE was then determined using the wave functions obtained from the self-consistent calculations. To obtain the MAE, the difference between energies E_{100} and E_{001} was evaluated. Here E_{100} and E_{001} are the total energies of the compounds with the corresponding magnetic moment orientations. A negative MAE value indicates easy plane anisotropy, while a positive value corresponds to easy axis anisotropy.

2. Results and discussions

This section discusses the results obtained for a set of $Mn_2Ni_{1+x}Ti_{1-x}$ alloys (x = 0, 0,25, 0,5 and 0,75). The procedure of geometrical optimization of Heusler crystal structures of $L2_1$, XA and T^p types was performed, taking into account their different magnetic ordering, to establish the energetically preferable structure for each compound. We would like to note that the T^p structure has been originally proposed by Neibecker *et al.* [16].

Fig. 2 clearly demonstrates the variations in total energy of the cubic structures based on their degree of tetragonal distortion c/a. It should be noted that the presence of a stable martensitic tetragonal phase in the alloy is indicated by a global energy minimum on the curve $E(c/a)$ at $c/a \neq 1$.

As can be seen from Fig. 2, *a*, for the stoichiometric compound Mn_2NiTi, layered atomic ordering of Ni and Mn is energetically favorable, thereby pointing to the T^p structure as the ground state of the austenite phase ($c/a \approx 1$), despite the fact that each of the structures exhibits pseudo-martensitic behavior at $c/a > 1$. The magnetic reference state of T^p structure is characterized by AFM* (layer-by-layer) ordering of the Mn spin moments. The energy difference between the T^p and XA, $L2_1$ structures with AFM* ordering is about 12,8 and 24,9 meV/atom, respectively. The FM solution for Mn_2NiTi is located signifi-

cantly higher on the energy scale, indicating its disadvantage. It should be noted that the XA and $L2_1$ structures have been experimentally observed in Heusler alloys, whereas the theoretical T^p structure has not been yet experimentally confirmed. Several theoretical papers [17-19] have reported the energetic favorability of the T^p structure for Fe- and Co-based Heusler alloys.

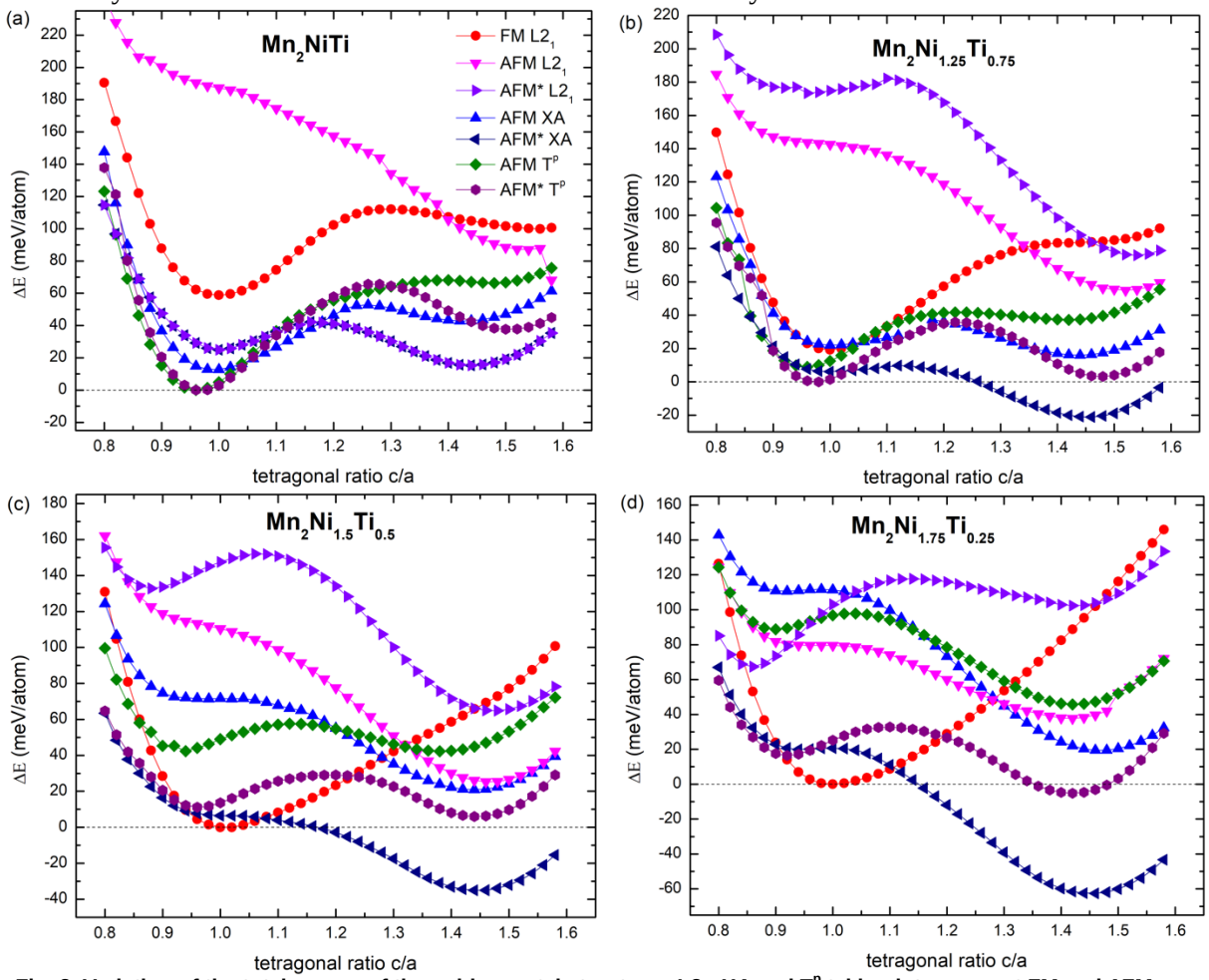

Fig. 2. Variation of the total energy of the cubic crystal structures $L2_1$, XA and T^p taking into account FM and AFM ordering as a function of the degree of their tetragonal distortion for $Mn_2Ni_{1+x}Ti_{1-x}$ alloys

Partial substitution of Ti atoms with excess Ni atoms results in a stable tetragonal phase with atomic ordering of the XA structure type (see Figs. 2, *b–d*). The layered antiferromagnetic ordering of Mn magnetic moments is energetically favorable in the martensitic phase for all non-stoichiometric compounds. In this case, the Mn atoms are located in two non-equivalent sublattices and are at the closest distance to the other atoms. It should be noted that an increase in the Ni content leads to a change in the ground state of the austenitic phase (c/a = 1). Thus, Fig. 2, *b* demonstrates that the T^p structure remains stable for the compound with x = 0,25, despite the smaller energy difference, $\Delta E \approx$ 6,42 meV/atom, between the AFM* T^p and AFM* XA structures compared to the value of $\Delta E \approx$ 12,8 meV/atom for Mn_2NiTi. Further increase in Ni content (x > 0,25) results in the instability of T^p structure for austenite phase. Similar finding has been reported recently for $FeNi_{2+x}Al_{1-x}$ alloys [17]. It is obvious from Fig. 2, *c*, *d* that an increase in x changes the atomic and magnetic ordering of the cubic austenite phase from AFM* T^p to FM $L2_1$ one. For the $L2_1$ structure, Mn atoms occupy equivalent positions at a greater distance ($d = 0{,}5a_0$) compared to the case of the T^p structure ($d = \sqrt{3}/4a_0$). An increase in the distance between Mn atoms causes a change in the nature of the magnetic interaction from AFM to FM.

The $E(c/a)$ curves for the $Mn_2Ni_{1+x}Ti_{1-x}$ compositions indicate that the martensitic transition temperature T_m will increase with increasing Ni content. This is a result of the heightened energy barrier between the cubic and tetragonal phases. Replacing Ti atoms with Ni atoms increases the concentration of valence electrons (e/a) per atom, resulting in a corresponding increase in the energy barrier with concentration x. This observation is consistent with the experimentally established linear dependence $T_m(e/a)$

[1–6]. The martensitic transition temperature can be roughly estimated using the relation: $\Delta E \approx k_B T_m$, where k_B is the Boltzmann constant. The temperature T_m for compositions with x = 0,25, 0,5 and 0,75 or with e/a = 7,375, 7,75 and 8,125, respectively, is calculated to be 245,9, 407,16, and 726,16 K, assuming ΔE of 21,2, 35,1, and 62,6 meV/atom, respectively.

Table 1 summarizes the equilibrium lattice parameters, total and elemental magnetic moments for the energetically favorable crystal structures of the compounds $Mn_2Ni_{1+x}Ti_{1-x}$, taking into account a magnetic reference ordering. The table clearly demonstrates that the equilibrium parameter of crystal structures in the austenitic phase increases as the Ni content increases. This is due to the larger atomic radius of Ni atoms compared to Ti atoms. However, the tetragonal structure parameters of the martensitic phase with XA ordering exhibit an ambiguous behavior that is dependent on the Ni content.

Table 1

Equilibrium lattice parameters (*a* and *c*), tetragonal ratio (*c*/*a*), total and elemental magnetic moments (μ_{tot} and μ_i) in [μ_B/f.u.] and [μ_B/at.], respectively, for $Mn_2Ni_{1+x}Ti_{1-x}$ alloys in cubic austenite and tetragonal martensitic phases. All parameters are presented for energetically favorable structures and magnetic configurations: AFM* T^p (*x* = 0 and 0,25), FM $L2_1$ (*x* = 0,5 and 0,75) for austenite; AFM* XA (*x* = 0,25, 0,5 and 0,75) for martensite

Compound	Parameters	x = 0	x = 0,25	x = 0,50	x = 0,75
austenite (c/a =1)	a	5,805	5,82	5,88	5,86
	μ_{tot}	3,275	2,657	6,87	7,817
	μ_{Mn1}	–0,282	–0,842	3,10	3,323
	μ_{Mn2}	2,975	2,992	3,10	3,323
	μ_{Ni}	0,475	0,434	0,796	0,821
martensite ($c/a \neq 1$)	a		5,130	5,136	5,113
	c		7,490	7,396	7,464
	c/a		1,46	1,44	1,46
	μ_{tot}		0,425	0,238	0,176
	μ_{Mn1}		2,509	2,688	2,981
	μ_{Mn2}		–2,217	–2,534	–2,865
	μ_{Ni}		0,027	0,032	0,009

The behavior of magnetic moments shows a clear trend: the total magnetization decreases for compositions with T^p structure and AFM* ordering of Mn_1 and Mn_2 atoms. This is a result of the increased magnetic moment of Mn_1 atoms located in the (002) plane, while Mn_2 atoms occupy tetrahedral positions in the T^p structure (see Fig. 1). Compounds with $L2_1$ ordering in the austenitic phase (x = 0,5 and 0,75) exhibit an increase in total magnetization. This is attributed to the growth of the element-by-element magnetic moments of Ni, Mn_1, and Mn_2 atoms. It is worth noting that the difference between Mn_1 and Mn_2 is purely conventional, as these atoms occupy equivalent positions in two interpenetrating FCC sublattices (refer to Fig. 1). The data clearly shows that as the Ni content increases, the total magnetization of the martensitic phase with XA ordering decreases significantly. This is due to the antiferromagnetic orientation of the magnetic moments of Mn_1 and Mn_2, which are located in non-equivalent positions (0, 0, 0) and (0,25, 0,25, 0,25) respectively (see Fig. 1). It is also worth noting that the magnetic moment of Ni atoms is suppressed. The binary compound Ni-Mn, resulting from the substitution of Ti for Ni, exhibits antiferromagnetism with a Neel temperature of around 1000 K [3, 20].

To calculate MAE, we chose the magnetic states of tetragonally distorted structures XA, $L1_0$, and T^p of $Mn_2Ni_{1+x}Ti_{1-x}$ compounds, as presented in Fig. 2, due to their close energy levels. Our selection of these structures was based on their energy levels and their suitability for accurate calculations. For the x = 0, we have considered the AFM* T^p (c/a = 0,96), and AFM* $L1_0$ (c/a = 1,44) structures. For the x = 0,25, we have taken the AFM* XA (c/a = 1,46), and AFM* T^p (c/a = 0,98) structures. Finally, for the x = 0,5 and x = 0,75, we have considered the AFM* XA (c/a = 1,44 and 1,46), and AFM* T^p (c/a = 1,44 and 1,42) structures, correspondingly.

Fig. 3 shows the histograms of MAE calculated for crystal structures mentioned above. Here, the negative sign of MAE indicates the energetically favorable in-plane spin direction and easy plane MAE, and vice versa the out-of-plane spin direction and easy axis MAE. For all compounds with tetragonally distorted AFM* XA and T^p structures, the easy-axis-type anisotropy is observed except Mn_2NiTi with tetragonal $L1_0$ structure, where the easy-plane-type anisotropy is preferable. In a case of compounds with x = 0 and 0,25, T^p structure with nearly cubic parameters (c/a = 0,96 and 0,98) demonstrates a considerable MAE, which is comparable with that of compounds with tetragonal structures (x = 0,5 and

0,75). The largest MAE value is calculated to be 0,4 MJ/m^3 for AFM* XA structure (c/a = 1,46) of $Mn_2Ni_{1,25}Ti_{0,75}$. However, for compounds with x = 0,5 and 0,75, the T^p structure reveals a larger values of MAE as compared to the XA structure. We would like to mentioned that the calculated values of MAE are comparable to those of $L1_0$-FeNi (0,22 – 0,48 MJ/m^3 [21–24]), which is the most intensely discussed candidate for high-performance rare-earth-free permanent magnets.

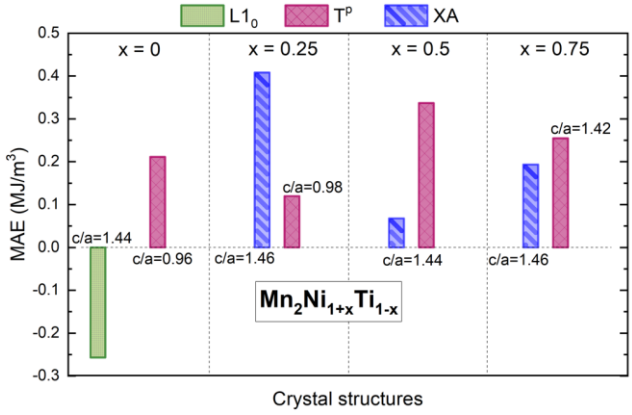

Fig. 3. Magnetocrystalline anisotropy energy diagram for tetragonally distorted $L1_0$, XA, and T^p structures of $Mn_2Ni_{1+x}Ti_{1-x}$ alloys (x = 0, 0,25, 0,5, and 0,75) with the favorable magnetic configurations

Conclusions

In summary, we have performed the *ab initio* investigations of the influence of atomic and magnetic ordering on the ground state energy and magnitude of magnetocrystalline anisotropy for Heusler alloys of the Mn-Ni-Ti family, which consist entirely of transition *d* metals. For stoichiometric compound Mn_2NiTi, an energetically favorable structure T^p with nearly cubic lattice parameters and layer-by-layer ordering of Mn and Ni atoms is predicted. This structure is characterized by the antiferromagnetic spin alignment of Mn magnetic moments. Furthermore, this structure demonstrates an easy-axis magnetocrystalline anisotropy of about 0,2 MJ/m^3, which is not typical of cubic phases. When Ti atoms are partially substituted with Ni, stable tetragonal structures T^p and XA emerge, which are ordered antiferromagnetically. An increase in Ni content results in a higher energy barrier between cubic and tetragonal phases, indicating a rise in the martensitic transition temperature. It was found that the $Mn_2Ni_{1,25}Ti_{0,75}$ compound in the tetragonal XA structure with c/a ratio of 1,46 exhibits the highest MAE value of 0,4 MJ/m^3. Nevertheless, for compounds with x = 0,5 and 0,75, the tetragonal T^p structure also exhibits larger MAE values compared to the XA structure. Overall, the MAE values obtained are comparable to those of tetratenite $L1_0$-FeNi, which is an alternative to rare-earth-free permanent magnets.

This study was supported by the Russian Science Foundation (RSF), Project No. 24-12-20016.

References

1. Krenke T., Duman E., Acet M., Wassermann E. F., Moya X., Mañosa L., Planes A. Inverse Magnetocaloric Effect in Ferromagnetic Ni–Mn–Sn Alloys. *Nat. Mater.*, 2005, Vol. 4, pp. 450–454. DOI: 10.1038/nmat1395.

2. Kainuma R., Imano Y., Ito W., Sutou Y., Morito H., Okamoto S., Kitakami O., Oikawa K., Fujita A., Kanomata T., Ishida K. Magnetic-Field-Induced Shape Recovery by Reverse Phase Transformation. *Nature*, 2006, Vol. 439, pp. 957–960. DOI: 10.1038/nature04493.

3. Entel P., Buchelnikov V.D., Gruner M.E., Hucht A., Khovailo V.V., Nayak S.K., Zayak A.T. Shape Memory Alloys: A Summary of Recent Achievements. *Mater. Sci. Forum*, 2008, Vol. 583, pp. 21–41. DOI: 10.4028/www.scientific.net/MSF.583.21.

4. Buchelnikov V.D., Vasiliev A.N., Koledov V.V., Taskaev S.V., Khovaylo V.V., Shavrov V.G. Magnetic Shape-Memory Alloys: Phase Transitions and Functional Properties. *Phys.-Uspekhi*, 2006, Vol. 49, p. 871. DOI: 10.1070/PU2006v049n08ABEH006081.

5. Graf T., Felser C., Parkin S.S.P. Simple Rules for the Understanding of Heusler Compounds. *Prog. Solid State Chem.*, 2011, Vol. 39, Iss. 1, pp. 1–50. DOI: 10.1016/j.progsolidstchem.2011.02.001.

6. Tavares S., Yang K., Meyers M.A. Heusler alloys: Past, Properties, New Alloys, and Prospects. *Prog. Mater. Sci.*, 2022, Vol. 132, p. 101017. DOI: 10.1016/j.pmatsci.2022.101017.

7. de Paula V.G., Reis M.S. All-*d*-Metal Full Heusler Alloys: A Novel Class of Functional Materials. *Chem. Mater.*, 2021, Vol. 33, P. 5483–5495. DOI: 10.1021/acs.chemmater.1c01012.

8. Bachagha T., Suñol J.J. All-*d*-Metal Heusler Alloys: A Review. *Metals*, 2023, Vol. 13, Iss. 1, p. 111. DOI: 10.3390/met13010111.

9. Ahn K. Ni-Mn Based Conventional Full Heusler Alloys, All-*d*-Metal Full Heusler Alloys, and Their Promising Functional Properties to Solid State Cooling by Magnetocaloric Effect. *J. Alloys. Compd.*, 2024, Vol. 978, p. 173378. DOI: 10.1016/j.jallcom.2023.173378.

10. Wei Z.Y., Liu E.K., Li Y., Han X.L., Du Z.W., Luo H.Z., Liu G.D., Xi X.K., Zhang H.W., Wang W.H., Wu G.H. Magnetostructural Martensitic Transformations with Large Volume Changes and Magnetostrains in All-*d*-Metal Heusler Alloys. *Appl. Phys. Lett.*, 2016, Vol. 109, P. 071904. DOI: 10.1063/1.4961382.

11. Wei Z.Y., Sun W., Shen Q., Shen Y., Zhang Y. F., Liu E. K., Liu J. Elastocaloric Effect of All-*d*-Metal Heusler NiMnTi(Co) Magnetic Shape Memory Alloys by Digital Image Correlation and Infrared Thermography. *Appl. Phys. Lett.*, 2019, Vol. 114, Iss. 10, p. 101903. DOI: 10.1063/1.5077076.

12. Yan H.L., Wang L.D., Liu H.X., Huang X.M., Jia N., Li Z.B., Yang B., Zhang Y.D., Esling C., Zhao X., Zuo L. Giant Elastocaloric Effect and Exceptional Mechanical Properties in an All-*d*-Metal Ni–Mn–Ti alloy: Experimental and Ab-Initio Studies. *Mater. Des.*, 2019, Vol. 184, p. 108180. DOI: 10.1016/j.matdes.2019.108180.

13. Kresse G., Furthmüller J. Efficient Iterative Schemes for *Ab Initio* Total-Energy Calculations using a Plane-Wave Basis Set. *Phys. Rev. B*, 1996, Vol. 54, Iss. 14, p. 11169. DOI: 10.1103/PhysRevB.54.11169.

14. Kresse G., Joubert D. From Ultrasoft Pseudopotentials to the Projector Augmented-Wave Method. *Phys. Rev. B*, 1999, Vol. 59, Iss. 3, p. 1758. DOI: 10.1103/PhysRevB.59.1758.

15. Perdew J.P., Burke K., Ernzerhof M. Generalized Gradient Approximation Made Simple. *Phys. Rev. B*, 1996, Vol. 77, Iss. 18, p. 3865. DOI: 10.1103/PhysRevLett.77.3865.

16. Neibecker P., Gruner M. E., Xu X., Kainuma R., Petry W., Pentcheva R., Leitner M. Ordering Tendencies and Electronic Properties in Quaternary Heusler Derivatives. *Phys. Rev. B*, 2017, Vol. 96, Iss. 16, p. 165131. DOI: 10.1103/PhysRevB.96.165131.

17. Sokolovskiy V., Miroshkina O. N., Buchelnikov V. D., Gruner M.E. Impact of Local Arrangement of Fe and Ni on the Phase Stability and Magnetocrystalline Anisotropy in Fe-Ni-Al Heusler Alloys. *Phys. Rev. Mater.*, 2022, Vol. 6, Iss. 2, p. 025402. DOI: 10.1103/PhysRevMaterials.6.025402.

18. Miroshkina O.N., Sokolovskiy V.V., Buchelnikov V. D., Gruner M.E. Electronic and Vibrational Properties of Fe_2NiAl and Co_2NiAl full Heusler Alloys: A First-Principles Comparison. *IEEE Trans. Magn.*, 2022, Vol. 58, Iss. 8, p. 2700105. DOI: 10.1109/TMAG.2022.3142849.

19. Sokolovskiy V., Miroshkina O.N., Sanosyan A., Baigutlin D., Buchelnikov V., Gruner M.E. Magnetic and Structural Properties of Co-Ni-Z (Z = Al, Ga, In, Sn) Heusler alloys: Effect of structural Motives and Chemical Disorder. *J. Magn. Magn. Mater.*, 2022, Vol. 546, p. 168728. DOI: 10.1016/j.jmmm.2021.168728.

20. Kren E., Nagy E., Pal L., Szabo P. Structures and Phase Transformations in the Mn-Ni System Near Equiatomic Concentration. *J. Phys. Chem. Sol.*, 1968, Vol. 29, Iss. 1, pp. 101–108. DOI: 10.1016/0022-3697(68)90259-X.

21. Edström A., Chico J., Jakobsson A., Bergman A., Rusz J. Electronic Structure and Magnetic Properties of L10 Binary Alloys. *Phys. Rev. B*, 2014, Vol. 90, Iss. 1, P. 014402. DOI: 10.1103/PhysRevB.90.014402.

22. Werwinski M., Marciniak W. *Ab Initio* Study of Magnetocrystalline Anisotropy, Magnetostriction, and Fermi Surface of L10 FeNi (Tetrataenite). *J. Phys. D*, 2017, Vol. 50, no. 49, P. 495008. DOI: 10.1088/1361-6463/aa958a.

23. Wu R., Freeman A. Spin–orbit Induced Magnetic Phenomena in Bulk Metals and their Surfaces and Interfaces. *J. Magn. Magn. Mater.*, 1999, Vol. 200, Iss. 1-3, P. 498. DOI: 10.1016/S0304-8853(99)00351-0.

24. Miura Y., Ozaki S., Kuwahara Y., Tsujikawa M., Abe K., Shirai M. The Origin of Perpendicular Magneto-Crystalline Anisotropy in L10–FeNi under Tetragonal Distortion. *J. Phys. Condens. Matter.*, 2013, Vol. 25, P. 106005. DOI: 10.1088/0953-8984/25/10/106005.

Received April 11, 2024

Information about the authors

Sokolovskiy Vladimir Vladimirovich is Dr. Sc. (Physics and Mathematics), Associate Professor, Chelyabinsk State University, Chelyabinsk, Russian Federation, e-mail: vsokolovsky84@mail.ru.

Buchelnikov Vasiliy Dmitrievich is Dr. Sc. (Physics and Mathematics), Professor, Chelyabinsk State University, Chelyabinsk, Russian Federation, e-mail: buche@csu.ru.

Cong Daoyong is Professor, Beijing University of Science and Technology, Beijing, People's Republic of China, e-mail: dycong@ustb.edu.cn.

Bulletin of the South Ural State University
Series "Mathematics. Mechanics. Physics"
2024, vol. 16, no. 2, pp. 78–85

УДК 538.911 **DOI: 10.14529/mmph240208**

МАГНИТНЫЕ И СТРУКТУРНЫЕ СВОЙСТВА СПЛАВОВ ГЕЙСЛЕРА MN-NI-TI, ПОЛНОСТЬЮ СОСТОЯЩИХ ИЗ ПЕРЕХОДНЫХ МЕТАЛЛОВ

В.В. Соколовский[1], В.Д. Бучельников[1], Д. Конг[2]
[1]*Челябинский государственный университет, Челябинск, Российская Федерация*
[2] *Пекинский научно-технический университет, Пекин, Китайская Народная Республика*
E-mail: vsokolovsky84@mail.ru

Аннотация. Представлены теоретические исследования влияния различного атомного и магнитного упорядочения на структурные и магнитные свойства сплавов $Mn_2Ni_{1+x}Ti_{1-x}$, полностью состоящих из переходных металлов. Используя теорию функционала плотности, мы предсказываем основные структурные и магнитные состояния соединений с x = 0, 0,25, 0,5 и 0,75 как в кубических аустенитных, так и в тетрагональных мартенситных фазах. Обнаружено, что частичное замещение атомов Ti на Ni приводит к увеличению энергетического барьера между структурными фазами, к смене слоевого атомного упорядочения на чередующееся шахматное, а также к переходу от антиферромагнитного к ферромагнитному упорядочению спинов в кубической фазе. Все соединения с тетрагонально искаженной структурой демонстрируют конфигурацию спинов вне плоскости и магнитокристаллическую анизотропию тппа «легкая ось», за исключением тетрагональной фазы $L1_0$ Mn_2NiTi. Для последней структуры наблюдается магнитная анизотропия типа «легкая плоскость». Рассчитанные значения анизотропии сравнимы с таковыми для тетрагонального $L1_0$-FeNi.

Ключевые слова: ab initio вычисления; сплавы Гейслера полностью состоящие из переходных металлов; атомное расположение; магнитокристаллическая анизотропия

Литература

1. Inverse Magnetocaloric Effect in Ferromagnetic Ni–Mn–Sn Alloys / T. Krenke, E. Duman, M. Acet *et al.* // Nat. Mater. – 2005. – Vol. 4. – P. 450–454.

2. Magnetic-Field-Induced Shape Recovery by Reverse Phase Transformation / R. Kainuma, Y. Imano, W. Ito et al. // Nature. – 2006. – Vol. 439. – P. 957–960. DOI: 10.1038/nature04493.

3. Shape Memory Alloys: A Summary of Recent Achievements / P. Entel, V.D. Buchelnikov, M.E. Gruner *et al.* // Mater. Sci. Forum. – 2008. – Vol. 583. – P. 21–41.

4. Магнитные сплавы с памятью формы: фазовые переходы и функциональные свойства / В.Д. Бучельников, А.Н. Васильев, В.В. Коледов // УФН. – 2006. – Т. 176, Вып.4. – С. 900–906.

5. Graf, T. Simple Rules for the Understanding of Heusler Compounds / T. Graf, C. Felser, S.S.P. Parkin // Prog. Solid State Chem. – 2011. – Vol. 39, Iss. 1. – P. 1–50.

6. Tavares, S. Heusler Alloys: Past, Properties, New Alloys, and Prospects / S. Tavares, K. Yang, M.A. Meyers // Prog. Mater. Sci. – 2022. – Vol. 132. – P. 101017.

7. de Paula, V.G. All-*d*-Metal Full Heusler Alloys: A Novel Class of Functional Materials / V.G. de Paula and M.S. Reis // Chem. Mater. – 2021. – Vol. 33. – P. 5483–5495.

8. Bachagha, T. All-*d*-Metal Heusler Alloys: A Review / T. Bachagha, J.J. Suñol // Metals. – 2023. – Vol. 13, Iss. 1. – P. 111.

9. Ahn, K. Ni-Mn Based Conventional Full Heusler Alloys, All-*d*-Metal Full Heusler Alloys, and Their Promising Functional Properties to Solid State Cooling by Magnetocaloric Effect / K. Ahn // J. Alloys. Compd. – 2024. – Vol. 978. – P. 173378.

10. Magnetostructural Martensitic Transformations with Large Volume Changes and Magnetostrains in All-*d*-Metal Heusler Alloys / Z.Y. Wei, E.K. Liu, Y. Li *et al.* // Appl. Phys. Lett. – 2016. – Vol. 109. – P. 071904.

11. Elastocaloric Effect of All-*d*-Metal Heusler NiMnTi(Co) Magnetic Shape Memory Alloys by Digital Image Correlation and Infrared Thermography / Z.Y. Wei, W. Sun, Q. Shen *et al.* // Appl. Phys. Lett. – 2019. – Vol. 114, Iss. 10. – P. 101903.

12. Giant Elastocaloric Effect and Exceptional Mechanical Properties in an All-d-Metal Ni–Mn–Ti alloy: Experimental and Ab-Initio Studies / H.L. Yan, L.D. Wang, H.X. Liu *et al.* // Mater. Des. – 2019. – Vol. 184. – P. 108180.

13. Kresse, G., Furthmüller J. Efficient Iterative Schemes for *Ab Initio* Total-Energy Calculations using a Plane-Wave Basis Set / G. Kresse, J. Furthmüller // Phys. Rev. B. – 1996. – Vol. 54, Iss. 14. – P. 11169.

14. Kresse, G. From Ultrasoft Pseudopotentials to the Projector Augmented-Wave Method / G. Kresse, D. Joubert // Phys. Rev. B. – 1999. – Vol. 59, Iss. 3. – P. 1758.

15. Perdew, J.P. Generalized Gradient Approximation Made Simple / J.P. Perdew, K. Burke, M. Ernzerhof // Phys. Rev. B. – 1996. – Vol. 77, Iss. 18. – P. 3865.

16. Ordering Tendencies and Electronic Properties in Quaternary Heusler Derivatives / P. Neibecker, M.E. Gruner, X. Xu *et al.* // Phys. Rev. B. – 2017. – Vol. 96, Iss. 16. – P. 165131.

17. Impact of Local Arrangement of Fe and Ni on the Phase Stability and Magnetocrystalline Anisotropy in Fe-Ni-Al Heusler Alloys / V. Sokolovskiy, O.N. Miroshkina, V.D. Buchelnikov, M.E. Gruner // Phys. Rev. Mater. – 2022. – Vol. 6, Iss. 2. – P. 025402.

18. Electronic and Vibrational Properties of Fe_2NiAl and Co_2NiAl full Heusler Alloys: A First-Principles Comparison / O.N. Miroshkina, V.V. Sokolovskiy, V.D. Buchelnikov, M.E. Gruner // IEEE Trans. Magn. – 2022. – Vol. 58, Iss. 8. – P. 2700105.

19. Magnetic and Structural Properties of Co-Ni-Z (Z = Al, Ga, In, Sn) Heusler alloys: Effect of Structural Motives and Chemical Disorder / V. Sokolovskiy, O.N. Miroshkina, A. Sanosyan *et al.* // J. Magn. Magn. Mater. – 2022. – Vol. 546. – P. 168728.

20. Structures and Phase Transformations in the Mn-Ni System Near Equiatomic Concentration / E. Kren, E. Nagy, L. Pal, P. Szabo // J. Phys. Chem. Sol. – 1968. – Vol. 29, Iss. 1. – P. 101–108.

21. Electronic Structure and Magnetic Properties of L10 Binary Alloys / A. Edström, J. Chico, A. Jakobsson *et al.* // Phys. Rev. B. – 2014. – Vol. 90, Iss. 1. – P. 014402.

22. Werwinski, M. *Ab Initio* Study of Magnetocrystalline Anisotropy, Magnetostriction, and Fermi Surface of L10 FeNi (Tetrataenite) / M. Werwinski, W. Marciniak // J. Phys. D. – 2017. – Vol. 50, no. 49. – P. 495008.

23. Wu, R. Spin–orbit Induced Magnetic Phenomena in Bulk Metals and their Surfaces and Interfaces / R. Wu, A. Freeman // J. Magn. Magn. Mater. – 1999. – Vol. 200, Iss. 1-3. – P. 498.

24. The Origin of Perpendicular Magneto-Crystalline Anisotropy in L10–FeNi under Tetragonal Distortion / Y. Miura, S. Ozaki, Y. Kuwahara *et al.* // J. Phys. Condens. Matter. – 2013. – Vol. 25. – P. 106005.

Поступила в редакцию 11 апреля 2024 г.

Сведения об авторах

Соколовский Владимир Владимирович – доктор физико-математических наук, доцент, Челябинский государственный университет, г. Челябинск, Российская Федерация, e-mail: vsokolovsky84@mail.ru.

Бучельников Василий Дмитриевич – доктор физико-математических наук, профессор, Челябинский государственный университет, г. Челябинск, Российская Федерация, e-mail: buche@csu.ru.

Конг Даоюн – профессор, Пекинский научно-технический университет, г. Пекин, Китайская Народная Республика, e-mail: dycong@ustb.edu.cn.